Available online at www.sciencedirect.com

SciVerse ScienceDirect

journal homepage: www.elsevier.com/locate/poamed

Review Article

# Current methods of focal liver lesion diagnosis

*Justyna Rembak-Szynkiewicz*[a], *Barbara Bobek-Billewicz*[a,*], *Maria Sokół*[b], *Marek K. Jurkowski*[c]

[a]*Department of Radiology, The Maria Sklodowska-Curie Memorial Cancer Center, Institute of Oncology, Gliwice Branch, Poland*
[b]*Department of Medical Physics, The Maria Sklodowska-Curie Memorial Cancer Center, Institute of Oncology, Gliwice Branch, Poland*
[c]*Department of Medical Analytics, University of Warmia and Mazury, Olsztyn, Poland*

ARTICLE INFO

*Article history:*
Received 21 January 2013
Received in revised form
25 April 2013
Accepted 11 September 2013
Available online 17 September 2013

*Keywords:*
MDCT
MRI
DW-MRI
Liver
Focal
Lesion

ABSTRACT

*Introduction:* The widespread availability of non-invasive radiological and diagnostic imaging techniques significantly contributed to the detectability of focal lesions in the liver. Ultrasonography, computed tomography (CT) multidetector CT (MDCT), conventional magnetic resonance imaging (MRI), diffusion-weighted magnetic resonance imaging (DW-MRI) and isotope imaging are used for focal liver diagnosis.

*Aim:* This article reviews the available methods for diagnosing focal liver lesions on the basis of current literature.

*Discussion:* The diagnostic precision of a conventional ultrasound test in detecting and differentiating focal hepatic lesions is estimated at 62%. Its sensitivity for the detection of metastases ranges from 40% to 80%. If the majority of metastatic tumors are small, the sensitivity of ultrasound tests decreases dramatically to 20% for foci smaller than 1 cm.

Multi-phase hepatic CT is the current standard that effectively diagnoses 63%–87% of focal changes in the liver. In many cases, standard MRI is sufficient for differentiating between benign and malignant tumors, but the results are often inconclusive. DW-MRI has emerged as a highly promising technique for oncological imaging, and it is used at various stages of oncological treatment.

The discussed method does not require the administration of intravenous contrast, therefore, it is easy to repeat and useful in patients who suffer from severe renal dysfunctions and are at the risk of nephrogenic systemic fibrosis.

In diagnosis of hepatic metastases, the sensitivity of 18F-FDG-PET/CT scans reaches up to 96%, and their specificity is estimated at 75%.

*Conclusions:* Among various imaging techniques diffusion-weighted imaging has emerged recently as a highly promising one.



*Correspondence to: Department of Radiology, The Maria Sklodowska-Curie Memorial Cancer Center, Institute of Oncology ul. Wybrzeże Armii Krajowej 15, 44-100 Gliwice, Poland. Tel.: +48 32 278 93 67; fax: +48 32 278 93 65.
*E-mail address:* bbillewicz@io.gliwice.pl (B. Bobek-Billewicz).

1230-8013/$ - see front matter © 2013 Warmińsko-Mazurska Izba Lekarska w Olsztynie. Published by Elsevier Urban & Partner Sp. z o.o. All rights reserved.
http://dx.doi.org/10.1016/j.poamed.2013.09.003

## 1. Introduction

The widespread availability of non-invasive radiological and diagnostic imaging techniques significantly contributed to the detectability of focal lesions in the liver. Accidentally detected benign tumors occur in around 15% of the healthy population,[24] and the probability that focal changes are malignant in persons with no cancer history does not exceed 1%.[13,24] It is estimated that around 20% of focal liver lesions (which are not simple cysts) observed in patients with malignancies are benign, but such changes are regarded as metastases until they are ruled out. Metastatic tumors account for 95% of all hepatic malignancies, while primary tumors for only 5%.

The liver is the second most common site of metastasis after regional lymph nodes.[16] In around 90% of cases, liver metastases are multifocal. The size of metastatic foci may vary, and it may exceed 10 cm. Lesions smaller than 2 mm are not detected by the available imaging methods.

Subject to the degree of vascularization, metastases are classified as richly or weakly vascularized. Richly vascularized (hypervascular) tumors are characterized by rapid, early contrast wash-in, and they are more enhanced that the remaining liver parenchyma in the arterial phase of dynamic magnetic resonance imaging (MRI) after intravenous contrast administration. Due to a higher wash-out rate, a rapid drop in signal intensity is observed in metastases in later phases of dynamic MRI (computed topography – CT), and ultimately, those lesions become hypointensive compared to a normal liver.

The more frequently encountered weakly vascularized metastases are characterized by low blood flow in the tumor, and their contrast enhancement remains low at all stages of a dynamic exam. Hypovascular metastases are most often caused by colorectal cancer, pancreatic cancer, lung cancer, pharyngeal carcinoma, melanoma, ovarian cancer, breast cancer, cervical cancer and liposarcoma. Infiltrations in non-Hodgkin lymphoma and Hodgkin lymphoma are also hypovascular.

The liver is also affected by benign tumors which are often very difficult to differentiate from malignant neoplasms. The most common benign lesions are cysts (5%–10% of the population), hemangiomas (5%–20%),[13,24] foci of fatty degeneration and focal nodular hyperplasia (around 3%). Less frequent benign tumors include adenomas (mostly in women using hormonal contraceptives, 3–4/100,000)[24] and abscesses. In most cases, hepatic metastases have to be differentiated from hemangiomas owing to their similar appearance in imaging tests and the high frequency of hemangioma occurrence.

## 2. Aim

This article reviews the available methods for diagnosing focal liver lesions on the basis of current literature.

## 3. Discussion

### 3.1. *Ultrasonography*

Ultrasonography with or without contrast agents is the most common and generally the first imaging method used to examine the parenchymal organs of the abdomen, including the liver. The diagnostic precision of a conventional ultrasound test in detecting and differentiating focal hepatic lesions is estimated at 62%.[13] Its sensitivity for the detection of metastases ranges from 40% to 80%,[9,13,31] subject to the tumor's diameter and the examiner's experience, and it rarely exceeds 80%. It should be noted, however, that the majority of metastatic tumors are small, and the sensitivity of ultrasound tests decreases dramatically to 20% for foci smaller than 1 cm.[13]

Intraoperative ultrasound (IOUS) imaging, which requires probes with a frequency of 7.5 MHz and higher, is characterized by improved spatial resolution, and it supports the detection of surface-located tumors with a diameter of only 2 mm.

Elastography is a new non-invasive technique that complements a basic ultrasound exam. This method has been most often applied to characterize breast tumors.[6] It is also used to examine patients with chronic liver diseases.

### 3.2. *Computed tomography*

A CT scan of the liver without the intravenous administration of contrast media has limited diagnostic value.[1] Multi-phase hepatic CT (MDCT) is the current standard that effectively diagnoses 63%–87% of focal changes in the liver.[25]

### 3.3. *Magnetic resonance imaging*

MRI is emerging as the most accurate method for detecting and differentiating focal liver lesions.[16,17,30] It provides better contrast between different soft tissues than CT, and the latest MRI scanners offer spatial and temporal resolution comparable with that of CT. MRI has a small number of absolute contraindications, such as a heart pacemaker, a metallic foreign body in the eye or cochlear implants.

Conventional MRI, including T1-weighted imaging with and without contrast enhancement, T2-weighted imaging, fat suppression sequences (SPAIR – spectral attenuation with inversion recovery, STIR – short T1 inversion recovery, chemical shift imaging) and MR angiography support determinations of the size and location of hepatic tumors (including in relation to blood vessels and bile ducts) and, to a certain extent, evaluations of tumor tissue composition. In many cases, standard MRI is sufficient for differentiating between benign and malignant tumors, but the results are often inconclusive.

MRI scans performed with the use of hepatotropic contrast agents which are captured and excreted by the hepatocytes support the differentiation of tumors which contain normal hepatocytes from lesions that do not contain hepatocytes or contain abnormal hepatocytes.

Hepatotropic contrast agents improve the detectability of small (<1 cm) focal liver lesions. In patients affected by renal failure, contrast agents containing gadolinium may cause nephrogenic systemic fibrosis (NSF); therefore, kidney function has to be examined before the administration of a contrast

agent.[11] A multi-phase contrast CT/MR examination generally involves three phases:

(1) early arterial phase (scan delay of 10 s) or arterial phase (delay of 15–25 s),
(2) portal venous phase (delay of 60 s),
(3) equilibrium phase (delay of 120 s after contrast administration or 180 s in patients with liver cirrhosis).[17,21,24]

MRI of the liver may be complemented by MR cholangiography which images the biliary tract and the pancreatic duct without the administration of a contrast medium. Since the development of MR cholangiography, endoscopic retrograde cholangiopancreatography (ERCP) has been used as a therapeutic rather than a diagnostic procedure.[27]

Conventional MRI techniques effectively differentiate between benign and malignant lesions only in some cases,[27] which is why new MRI methods offering enhanced soft-tissue visibility are researched (Table 1).

### 3.4. *Diffusion-weighted MRI*

Diffusion-weighted MRI (DW-MRI) makes use of the motion of water molecules within extracellular/extravascular space. In biological systems, diffusion is influenced by the shape and size of extracellular space, the properties of cell membranes, the content of macromolecules as well as the exchange of water between the intracellular and the extracellular compartment. The shape and the size of extracellular space are determined mainly by the size, arrangement and density of cells.[12,14,22] DW-MRI provides information about tissue architecture and, indirectly, about the microstructure of the examined tissues.[12,14]

Diffusion of water molecules also takes place inside the cell (where it is determined by the size and number of intracellular structures and the amount of cytoplasm), but this process has a negligible effect on MR water diffusion imaging.

Blood flow and perfusion, heart pulse and respiratory movements influence the observed motion of water molecules, and they can reduce the accuracy of water diffusion measurements.[12,14,22] Blood flow in microcapillaries mimics diffusion, and it has the most profound effect on DW images at low values of the *b*-factor ($b \leq 100$ s/mm$^2$).[12,14]

DW-MRI is a spin-echo sequence or a gradient-echo sequence which contains an extra pair of gradients, i.e. diffusion gradients.[14] Signal intensity (SI) in DW images reflects the net movement of spins and its attenuation depends on the magnitude of molecular translation and diffusion weighting. The latter is determined by the strength of the diffusion gradients, the duration of the gradients, and the time between the gradient pulses.

The parameter that summarizes the influence of the gradients on the diffusion weighted images is the *b*-factor (s/mm$^2$), which is given by the following formula:

$$b = \gamma^2 G^2 \delta^2 (\Delta - \delta/3)$$

where $\gamma$ is the gyromagnetic ratio, $G$ the amplitude of the two diffusion gradient pulses, $\delta$ the duration of the pulses, $\Delta$ the time between the two pulses.

Thus, the ratio of diffusion-weighted signal to non-diffusion-weighted signal is

$$S/S_0 = \exp(-\gamma^2 G^2 \delta^2 (\Delta - \delta/3) D) = \exp(-bD)$$

where $S_0$ is the signal intensity without the diffusion weighting, $S$ the diffusion-weighted signal and $D$ the diffusion coefficient (a measure of the strength (velocity) of diffusion in tissue; the stronger the diffusion, the greater the diffusion coefficient, i.e. the apparent diffusion coefficient – APC).

In DW-MRI examinations, the lowest *b*-value is nearly always 0 s/mm$^2$ (less frequently 50 s/mm$^2$), and the highest *b*-value is noted in the range of 750 s/mm$^2$ to 1000–1400 s/mm$^2$.[7,12,14,20,22] The successive parts of the sequence are images acquired at $b>0$. The data obtained from measurements of at least two diffusion acquisitions at different *b*-values support quantitative measurements of the mobility (diffusion) of water molecules. A measure of molecule mobility is the ADC which is expressed in mm$^2$/s.

$$ADC = -\frac{1}{b_1 - b_0} \ln\left(\frac{S}{S_0}\right)$$

where $b_1$ is the value of *b*-factor, $b_0$ the value of *b*-factor without the use of gradients, T2 the weighted image, $S$ the diffusion-weighted signal, $S_0$ the signal intensity without the diffusion weighting.

Directional and index DW images contain elements of images dependent on diffusion and relaxation time T2, but in ADC maps, the T2 shine-through effect is eliminated.[14,26] Changes in water diffusion in tissues analyzed by DW-MRI result mainly from variations in the volume of extracellular space. A reduction in extracellular space can be caused by an increase in cell volume (as observed in, for example, cytotoxic swelling) or an increase in the number of cells or macromolecules per unit volume (as observed in, for example, tumors and abscesses). The above contributes to a phenomenon known as restricted diffusion.[2,14,22,28]

DW-MRI does not require the administration of intravenous contrast; therefore, it is easy to repeat and useful in patients who suffer from severe renal dysfunctions and are at the risk of nephrogenic systemic fibrosis.

Malignant tumors generally restrict diffusion, and the ADC of malignancies is clearly lower than that of benign lesions.[1,2,7,8,10,14,20] In malignant tumors, high cellular density, disorganized tissue structure and greater irregularity of extracellular space decrease the mobility of water molecules and restrict diffusion, and such tissues are characterized by high signal intensity in DW images with high *b*-values and low values of ADC.[12,14,22]. An absence of restricted diffusion is generally regarded as an indication of non-malignant lesions. Generally, in high *b*-value DW images, benign lesions are isointense in comparison with healthy organs, and they are characterized by high SI in ADC maps[12,14,22,28] (Figs. 1 and 2, Table 2).

The accuracy of DWI is determined by various factors, mostly tumor size and the structure of tumors and organs, as well as the applied technique and patient cooperation. In organs with a specific structure, such as the spleen, tonsils or testes, the diffusion of water molecules is impaired. Differences in diffusion are too small to support correct imaging of

**Table 1 – Most frequent characteristics of focal liver lesions displayed by different imaging techniques.**

| Focal lesion | USG | CT without contrast | MR | | | Dynamic examination after intravenous contrast administration | | | |
|---|---|---|---|---|---|---|---|---|---|
| | | | T1-W images | T2-W images | Change of SI in phase/contraphase | Aortic phase CT/MR | Portal phase CT/MR | Equilibrium phase CT/MR | Hepatic-cellular phase MR |
| Cyst | Apnea | ↓ | ↓ | ↑ | No | **No enhancement** Hypodensive, hypointensive | **No enhancement** Hypodensive, hypointensive | **No enhancement** Hypodensive, hypointensive | **No enhancement** Hypodensive, hypointensive |
| Hemangioma | ↑ | ↓ | ↓ | ↑ | No | **Strong, mostly peripheral** Small n – homogenous Hyperdensive/ hyperintensive | **Progressive enhancement from periphery** Hyperdensive/ hyperintensive | **Progressive enhancement from periphery** Hyper/isodensive Hyper/isointensive | Hypointensive |
| FNH | ↓↔ **Central scar** | ↓ ↔ | ↓ ↔ | ↑↔ | No | **Strong (no scar)** Hyperdensive, hyperintensive | Isodensive/ isointensive (hypointensive scar) | Iso/hyperdensive Iso/hyperintensive (scar enhancement) | Iso/ hyperintensive (hypointensive scar) |
| Adenoma | ↔↓ **Frequently non-homogenous** | ↓↑ ↔ | ↔↑ ↑ | ↔↑ | Yes | **Quite strong** Hyperdensive/ hyperintensive | Isodensive/ isointensive | Isodensive/ isointensive | Hypo/ isointensive |
| HCC | ↓ | ↓ | ↑↓ | ↑ | Yes | **Quite strong** Hyperdensive/ hyperintensive | Hypo/isodensive Hypo/ isointensive | Hypo/isodensive Hypo/isointensive | Hypo/ isointensive |
| Hypervascular metastasis | ↓↑ | ↓ | ↓ | ↑ | Yes | **Strong** Hyperdensive/ hyperintensive | Hypo/isodensive, hypo/ isointensive | Hypodensive, hypointensive | Hypointensive |
| Hypovascular metastasis | ↑↓ | ↓ | ↓ | ↑ | No | **Weak/ peripheral** Hyperdensive, hyperintensive | Hyperdensive, hyperintensive | Hypodensive, hypointensive | Hypointensive |

↓ – SI/density/focal lesion echogenicity lower than in a normal liver.
↑ – SI/density/focal lesion echogenicity higher than in a normal liver.
↔ – SI/density/focal lesion echogenicity similar to a normal liver.

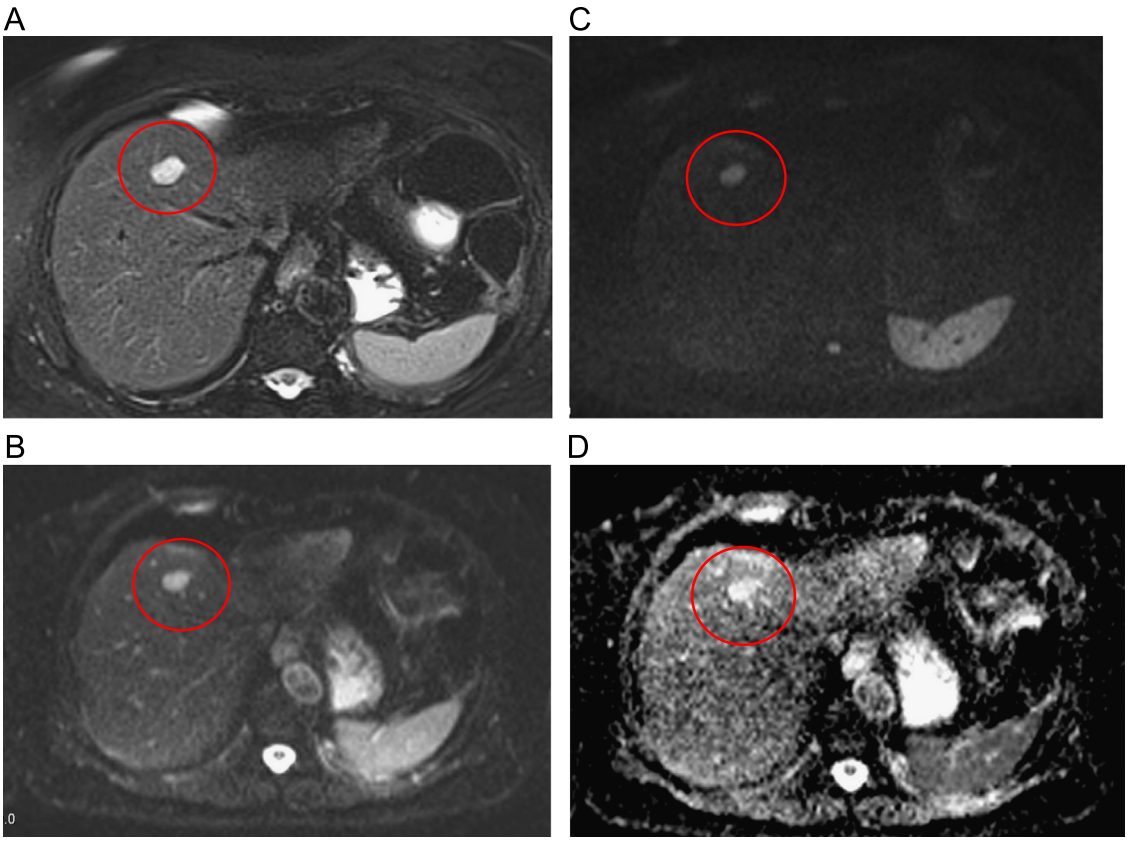


**Fig. 1 – Liver hemangioma (patient, female, age: 54). DWI – no diffusion limitation (high SI in DWI $b_{high}$ (C) +high ADC, (D) – red circle). (A) DWI $b=0$ s/mm$^2$ – high SI of hemangioma, (B) DWI $b=50$ s/mm$^2$ – high SI of hemangioma, (C) DWI $b=1000$ s/mm$^2$ – high SI of hemangioma, (D) ADC map – high ADC of hemangioma.**

neoplastic infiltrations in those organs. In some organs or their parts, such as the left lobe of the liver, respiratory motion and vascular pulsation artifacts may be observed.[12,14,22,28,29]

A *b*-value of 0 s/mm$^2$ delivers a T2-weighted echo-planar imaging scans image where DW images are T2-weighted images where venous vessels, similarly to the majority of focal lesions, are characterized by high SI; therefore, some small lesions (<1 cm) in the liver parenchyma may be undetected. When *b*-value falls in the range of 50–150 s/mm$^2$, the signal intensity of liver vessels is attenuated, and the signal intensity of most focal lesions, both benign and malignant, remains high which, with a relatively high value of SNR, supports imaging of very small lesions.[4,14] (Table 3).

Effective cancer treatment leads to tumor cell damage, loss of cell membrane integrality and an increase in extracellular space, which generally enhances free diffusion of water molecules in neoplastic tissue and increases ADC values.[5,14,18,23] A drop in ADC values may also be encountered in early stages of treatment, and it is attributed to cell swelling. DWI is most effective at diagnosing the early response to the treatment of breast cancer, brain tumors, primary and secondary liver cancer and bone cancer. According to Padhani, DWI differentiates between ischemic but still functioning tissues and necrotized tissues during treatment with combrestatin which damages blood vessels in tumors.[22] DWI/ADC images are also used to evaluate the response to radiation therapy and the effectiveness of non-invasive treatment of liver malignancies, such as transcatheter arterial chemoembolization (TACE) and tumor ablation (RFA, MVA, HIFU, cryoablation).[14,18,22]

Differentiation of post-treatment lesions from neoplastic infiltrations often poses a diagnostic problem. Unrestricted diffusion practically rules out infiltration,[14,22] and it points to post-radiotherapy swelling of tissue or an inflammatory process. Restricted diffusion, especially if accompanied by pathological contrast enhancement, is more indicative of neoplastic infiltration or a relapse.[14,22] Post-treatment fibrosis or dehydration are characterized by low ADC values, but most misdiagnoses can be eliminated by evaluating DW images together with ADC maps. In this respect, DW-MRI appears superior to FDG PET/CT, because shortly after radiotherapy, treatment-induced inflammations often augment glucose uptake, which could produce false positive results in a PET/CT scan, but they do not restrict diffusion.[12,14,22]

Diagnostic procedures proposed for focal lesion in the liver, uncharacteristic in ultrasonography, CT and MRI, are presented in Table 4.

### 3.5. *Isotope imaging*

The key isotope method for liver imaging is PET/CT with 18 FDG or ($^{68}$Ga)-labeled somatostatin analogs and somatostatin receptor-based scintigraphy (SPECT). In diagnoses of hepatic metastases, the sensitivity of 18F-FDG-PET/CT scans reaches up to 96%, and their specificity is estimated at 75%.[3] Somatostatin receptor-based scintigraphy relies on synthetic

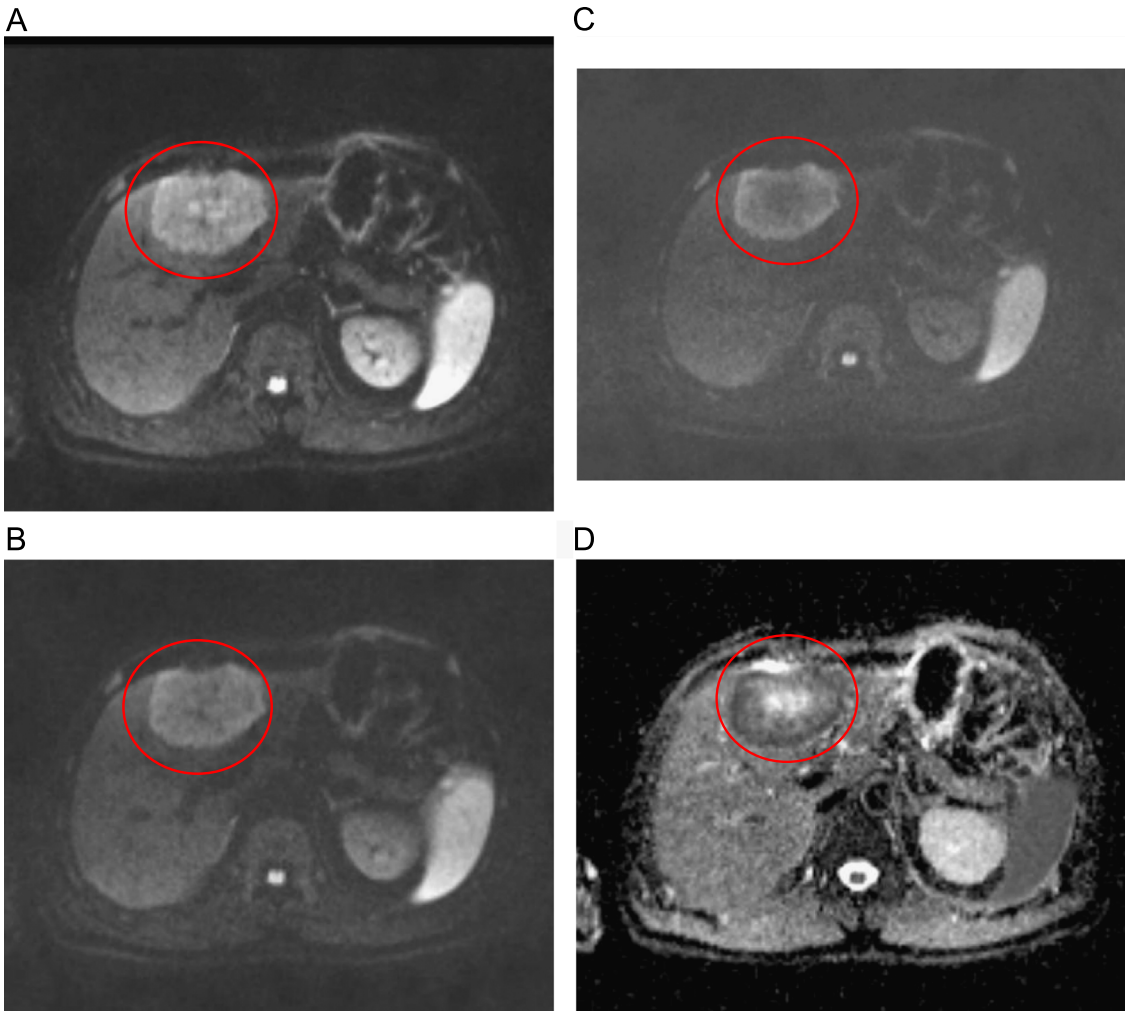


**Fig. 2 – Liver metastases from colon cancer (patient, male, age: 64). DWI MR – limited diffusion (high SI in DWI $b_{high}$ (C) +low ADC (D) – red circle). (A) DWI $b=50$ s/mm$^2$ – increased SI of metastasis, (B) DWI $b=600$ s/mm$^2$ – non-homogenously increased SI of metastasis, (C) DWI $b=1000$ s/mm$^2$ – SI of metastasis increased on the periphery and decreased in the center, (D) ADC map – low ADC value on the periphery of metastasis – limited diffusion; high ADC value in the central part – accelerated diffusion, necrotic lesions.**

**Table 2 – Interpretation of DW-MR images.[22]**

| T2-weighted image | DW image, $b_{high}$ | ADC | Interpretation |
|---|---|---|---|
| ↑↔ | ↑ | ↓ | Hypercellular tumor, coagulation necrosis, abscess |
| ↑ | ↑ | ↑ | T2-shine-through effect protein-rich fluid |
| ↑↔ | ↓ | ↓ | Fibrous tissue with a small amount of water/without tumor cells |
| ↑ | ↓ | ↑ | Fluid colliquative necrosis hypocellular tumor glandular structure |

**Table 3 – DWI/ADC images of the most common liver focal lesions.**

| Focal lesion | DWI, $b_{high}$ | ADC | Restricted diffusion |
|---|---|---|---|
| Cyst | Low SI | High | No |
| Hemangioma | High SI | High | No |
| Focal nodular hyperplasia | Low/high SI | High/low | No/yes |
| Adenoma | Low/high SI | High/low | No/yes |
| Abscess – central part – capsule | High SI | Low | Yes |
| | Low SI | Low | No |
| Metastasis | High SI | Low | Yes |
| Hepatocellular carcinoma (average and poorly differentiated) | High SI | Low | Yes |
| Hepatocellular carcinoma (well differentiated) | Moderate/low SI | Low | Yes/no |

**Table 4 – Diagnostic procedures propositions for focal lesion in the liver, uncharacteristic in US, CT and MRI.**

| | Focal lesion in the liver, uncharacteristic in ultrasonography, CT and MRI | Proposed follow up/biopsy algorithm | Proposed additional examinations to obtain the diagnosis |
|---|---|---|---|
| 1. | **Probably atypical hemangioma**<br>– Patient without known malignant disease | **US** follow up (possibly CT or MRI f/u):<br>– In 3 months<br>– In 6 months<br>– In 12 months | – Scintigraphy with Tc marked erythrocytes<br>**Tc-99 m RBC** (when lesion >1 cm) |
| 2. | **Probably atypical hemangioma**<br>– Patient with known malignant disease (main differential diagnosis with a metastasis) | **CT** or **MRI** f/u:<br>– In 3 months<br>– In 6 months | – Scintigraphy with Tc marked erythrocytes<br>**Tc-99 m RBC**<br>– **18 FDG PET/CT** |
| 3. | Atypical solid nodule. Differential **diagnosis between FNH and adenoma** (high probability of a benign lesion) | **CT** or **MRI** f/u:<br>– In 3months<br>– In 6 months<br>– In 12 months<br>– **Core needles biopsy** | – MRI with liver-specific contrast agent |
| 4. | Atypical solid nodule: patient without liver cirrhosis. Differential **diagnosis between adenoma, HCC or metastasis** (high probability of a malignant lesion) | – **Core needles biopsy** (if negative, then surgical biopsy)<br>– **Surgical biopsy**<br>– If biopsies negative: CT or MRI f/u in 3 months | – MRI with liver-specific contrast agent<br>– **18 FDG PET/CT** |
| 5. | **Atypical solid nodule in the cirrhotic liver** | – **Core needles biopsy**<br>– **Surgical biopsy**<br>If biopsies negative CT or MRI f/u in 3 months | – MRI with liver-specific contrast agent |
| 6. | Atypical cystic-solid nodule. Differential **diagnosis between HCC, metastasis vs abscess** | – **Surgical biopsy** | **MRI+DWI** |

somatostatin analogs which accumulate in neuroendocrine tumors. According to numerous studies, scintigraphy with technetium-labeled red blood cells (Tc-99m RBC) has 99% specificity for the detection of hemangiomas,[19] but owing to the discussed method's low spatial resolution, its specificity for tumors smaller than 2 cm is considerably lower.

## 4. Conclusion

Among various imaging techniques DWI has emerged recently as a highly promising one.

## Conflict of interest

None declared.

REFERENCES

[1] Bruegel M, Holzapfel K, Gaa J, Woertler K, Waldt S, Kiefer B, et al. Characterization of focal liver lesions by ADC measurements using a respiratory triggered diffusion-weighted single-shot echo-planar MR imaging technique. *Eur Radiol*. 2008;18 (3):477–485.

[2] Bruegel M, Rummeny EJ. Hepatic metastases: use of diffusion-weighted echo-planar imaging. *Abdom Imaging*. 2010;35 (4):454–461.

[3] Chua SC, Groves AM, Kayani I, Menezes L, Gacinovic S, Du Y, et al. The impact of 18F-FDG PET/CT in patients with liver metastases. *Eur J Nucl Med Mol Imaging*. 2007;34(12): 1906–1914.

[4] Coenegrachts K, De Geeter F, Ter Beek L, Walgraeve N, Bipat S, Stoker J, et al. Comparison of MRI (incliding SS SE-EPI end SPIO-enhanced MRI) and FDG–PET/CT for the detection of colcorectal metastases. *Eur Radiol*. 2009;19(2):370–379, http://dx.doi.org/10.1007/s00330-008-1163-y.

[5] Cui Y, Zhang X. Apparent diffusion coefficient: potential imaging biomarker for prediction and early detection of response to chemotherapy in hepatic metastases. *Radiology*. 2008;248(3):894–900, http://dx.doi.org/10.1148/radiol.2483071407.

[6] Fujimoto K, Kato M, Wada S. Non invasive evaluation of hepatic fibrosis in patients with chronic hepatitis C using elastography. *Medix*. 2007(suppl):24–28.

[7] Gourtsoyianni S, Papanikolaou N, Yarmenitis S. Respiratory gated diffusion-weighted imaging of the liver:value of apparent diffusion coefficient measurements in the differentiation between most commonly encountered benign and malignant focal liver lesions. *Eur Radiol*. 2008;18 (3):486–492.

[8] Holzapfel K, Bruegel M, Eiber M, Rummeny E, Gaa J. Detection and characterization of focal liver lesions using respiratory – triggered diffusion – weighted MR imaging (DWI). *MAGNETOM Flash*. 2008;2:6–9.

[9] Janica JR, Lebkowska U, Ustymowicz A. Contrast-enhanced ultrasonography in diagnosing liver metastases. *Med Sci Monit*. 2007;13(suppl 1):111–115.
[10] Kandpal H, Sharma R, Madhusudhan KS, Kapoor K. Respiratory – triggered versus breath-hold diffusion-weighted MRI of liver lesions: comparison of image quality and apparent diffusion coefficient values. *Am J Roentgenol*. 2009;192(4):915–922, http://dx.doi.org/10.2214/AJR.08.1260.
[11] Kendrick-Jones JC, Voss DM, De Zoysa JR. Nephrogenic systemic fibrosis in patients with end-stage kidney disease on dialysis, in the greater Auckland region, from 2000–2006. *Nephrology*. 2011;16(2):243–248, http://dx.doi.org/10.1111/j.1440-1797.2010.01397.x.
[12] Koh DM, Collins DJ. Diffusion-weighted MRI in the body: applications and challenges in oncology. *Am J Roentgenol*. 2007;188(6):1622–1635.
[13] Koh DM, Brown G, Riddell AM, Scurr E, Collins DJ, Allen SD, et al. Detection of corolectal hepatic metastases using MnDPDP MR imaging and diffusion-weighted imaging (DWI) alone and in combination. *Eur Radiol*. 2008;18(5):903–910, http://dx.doi.org/10.1007/s00330-007-0847-z.
[14] Koh DM, Thoeny HC, eds. *Diffusion-Weighted MR Imaging, Applications in the Body*. New York: Springer-Verlag; 2010.
[16] Lencioni R, ed. *Enhancing the Role of Ultrasound with Contrast Agents*. Italia: Springer-Verlag; 2006.
[17] Malone D, Zech Ch. Magnetic resonance imaging of the liver: consensus statement. *Eur Radiol*. 2008;18(suppl 4):D1–D16.
[18] Marugami N, Tanaka T, Kitano S. Early detection of therapeutic response to hepatic arterial infusion chemotherapy of liver metastases from colorectal cancer using Diffusion-Weighted MR Imaging. *Cardiovasc Intervent Radiol*. 2009;32(4):638–646, http://dx.doi.org/10.1007/s00270-009-9532-8.
[19] Morton KA, Clark PB, Christensen CR, O'Malley JP, Blodgett TM, Waxman A, et al. Diagnostic Imaging –Nuclear Medicine. *Pittsburg Amirsys*. 2007;1:8–42.
[20] Muhi A, Ichikawa T. High-*b*-value diffusion-weighted MR imaging of hepatocellular lesions: estimation of grade of malignancy of hepatocellular carcinoma. *J Magn Reson Imaging*. 2009;30(5):1005–1011, http://dx.doi.org/10.1002/jmri.21931.
[21] Optimized workflow of liver MRI, Bayer Schering Pharma AG. 2009.
[22] Padhani A, Liu G, Koh MD, Chenevert TL, Thoeny HC, Takahara T, et al. Diffusion-weighted magnetic resonance imaging as a cancer biomarker: consensus and recommendations. *Neoplasia*. 2009;11(2):102–125.
[23] Padhani A, Khan A. Diffusion-weighted (DW) and dynamic contrast-enhanced (DCE) magnetic resonance imaging (MRI) for monitoring anticancer therapy. *Targ Oncol*. 2010;5(1):39–52, http://dx.doi.org/10.1007/s11523-010-0135-8.
[24] Prokop M. *Spiralna i wielorzędowa tomografia komputerowa człowieka [Spiral and Multislice Computed Tomography of the Body]*. Warszawa: Medipage. 2007:403–470.
[25] Raman S, Leary C, Bluemke D, Amendola M, Sahani D, McTavish JD, et al. Improved characterization of focal liver lesions with liver-specific gadoxetic acid disodium-enhanced magnetic resonance imaging; a multicentre phase 3 clinical trail. *J Comput Assist Tomogr*. 2010;34(2):163–172, http://dx.doi.org/10.1097/RCT.0b013e3181c89d87.
[26] Rumuński J,Kalicka R,Bobek-Billewicz B. *Obrazowanie parametryczne w badaniach mózgu metodami MRI/PET [Synthesis and integration of parametric images in dynamic brain studies using PET–MRI]*. Gdańsk: Wydawnictwo Gdańskie. 2006:270–289.
[27] Runge V. *Rezonans magnetyczny w praktyce klinicznej. [MR in clinical practics]*. Urban Partner. 2007:291–316.
[28] Taouli B, Koh DM. Diffusion-weighted MR imaging of the liver. *Radiology*. 2010;254(1):47–66, http://dx.doi.org/10.1148/radiol.09090021.
[29] Taouli B, Koh DM. *Extra-Cranial Application of Diffusion-Weighted MRI*. New York: Cambridge University Press; 2011:18–31.
[30] Van der Slius F, Bosch J, Terkivatan T, de Man RA, Ijzermans JN, Hunink MG. Hepatocellular adenoma: costeffectiveness of different treatment strategies. *Radiology*. 2009;252(3):737–746, http://dx.doi.org/10.1148/radiol.2523082219.
[31] Yarmenitis SD, Karantanas A, Bakantaki Y. Detection od colorectal cancer hepatic metastases with kontrast-enhanced ultrasound: comparison with conventional B-Mode ultrasound. *Dig Dis*. 2007;25(1):86–93.

## Suggested for further reading

[15] Kwee T, Takahara T, Niwa T, Ivancevic MK, Herigault G, Van Cauteren M, et al. Influence of cardiac motion on diffusion-weighted magnetic resonance imaging of the liver. *Magn Reson Mater Phys*. 2009;22(5):319–325.